The Astrophysical Journal Letters, 771:L20 (5pp), 2013 July 10 doi:10.1088/2041-8205/771/2/L20

A SEARCH FOR C II 158 μm LINE EMISSION IN HCM 6A, A Lyα EMITTER AT $z = 6.56$

Nissim Kanekar[1,6], Jeff Wagg[2,3], Ranga Ram Chary[4], and Christopher L. Carilli[5]
[1] National Centre for Radio Astrophysics, Tata Institute of Fundamental Research, Pune 411 007, India; nkanekar@ncra.tifr.res.in
[2] European Southern Observatory, Alonso de Córdova 3107, Vitacura, Casilla 19001, Santiago 19, Chile
[3] Astrophysics Group, Cavendish Laboratory, University of Cambridge, Cambridge CB3 0HE, UK
[4] U.S. Planck Data Center, MS220-6 Caltech, Pasadena, CA 91125, USA
[5] National Radio Astronomy Observatory, P.O. Box O, Socorro, NM 87801, USA
Received 2013 March 8; accepted 2013 May 22; published 2013 June 20

ABSTRACT

We report a Plateau de Bure Interferometer search for C II 158 μm emission from HCM 6A, a lensed Lyα emitter (LAE) at $z = 6.56$. Our non-detections of C II 158 μm line emission and 1.2 mm radio continuum emission yield 3σ limits of $L_{\rm C\,II} < 6.4 \times 10^7 \times (\Delta V/100\ {\rm km\ s^{-1}})^{1/2}\ L_\odot$ for the C II 158 μm line luminosity and $S_{1.2\,\rm mm} < 0.68$ mJy for the 1.2 mm flux density. The local conversion factor between $L_{\rm C\,II}$ and the star formation rate (SFR) yields an SFR $< 4.7\ M_\odot\ {\rm yr^{-1}}$, $\approx$2 times lower than that inferred from the ultraviolet (UV) continuum, suggesting that the local factor may not be applicable in high-z LAEs. The non-detection of 1.2 mm continuum emission yields a total SFR $< 28\ M_\odot\ {\rm yr^{-1}}$; any obscured star formation is thus within a factor of two of the visible star formation. Our best-fit model to the rest-frame UV/optical spectral energy distribution of HCM 6A yields a stellar mass of $1.3 \times 10^9\ M_\odot$ and an SFR of $\approx 10\ M_\odot\ {\rm yr^{-1}}$, with negligible dust obscuration. We fortuitously detect CO $J = 3$–2 emission from a $z = 0.375$ galaxy in the foreground cluster A370, and obtain a CO line luminosity of $L'({\rm CO}) > (8.95 \pm 0.79) \times 10^8$ K km s^{-1} pc^2 and a molecular gas mass of $M({\rm H_2}) > (4.12 \pm 0.36) \times 10^9\ M_\odot$, for a CO-to-H$_2$ conversion factor of $4.6\ M_\odot\ ({\rm K\ km\ s^{-1}\ pc^2})^{-1}$.

Key words: cosmology: observations – galaxies: evolution – galaxies: formation – infrared: galaxies

Online-only material: color figure

1. INTRODUCTION

A large population of Lyα emitters (LAEs) have recently been detected at $z \gtrsim 6$, toward the end of the epoch of reionization (e.g., Hu et al. 2002a; Taniguchi et al. 2005; Kashikawa et al. 2011). LAEs appear to be normal star-forming galaxies, with star formation rates (SFRs) of $\approx$5–60 $M_\odot\ {\rm yr^{-1}}$. Their space density is sufficiently high that low-luminosity LAEs may be the primary source of the ultraviolet (UV) photon background required for reionization (Kashikawa et al. 2011). Detailed studies of the high-z LAE population are hence of much interest.

At high redshifts, $z > 6$, and for massive galaxies and quasars, radio CO lines have proven good tracers of the gas associated with star formation (e.g., Walter et al. 2003; Wang et al. 2010, 2011). Unfortunately, deep CO searches in LAEs at similar redshifts ($z \sim$ 6.5–7) have so far only yielded non-detections (Wagg et al. 2009; Wagg & Kanekar 2012).

The C II 158 μm $^2P_{3/2} \rightarrow {}^2P_{1/2}$ transition is one of the brightest lines in the spectrum of any galaxy, often carrying $\approx$0.5% of the total galaxy luminosity (e.g., Crawford et al. 1985; Stacey et al. 1991). It is the primary coolant of the diffuse interstellar medium at temperatures <5000 K (e.g., Wolfire et al. 1995) and is thus an excellent tracer of cold neutral gas, the fuel for star formation. While C II 158 μm emission has long been known to arise from photodissociation regions (e.g., Crawford et al. 1985), the C II 158 μm emission from extended diffuse gas in normal galaxies has been recently shown to be comparable to that from dense star-forming regions (Pierini et al. 2001). C II 158 μm emission studies may thus also provide information on the kinematics and dynamical masses of high-z galaxies, besides the spatial distribution of star-forming gas.

The C II 158 μm transition thus provides a useful tracer of physical conditions in $z > 6$ star-forming galaxies (e.g., Carilli & Walter 2013). While C II 158 μm emission has been found in a number of star-forming galaxies at $z \approx 1.2$ (Stacey et al. 2010), most high-z ($z \gtrsim 4$) searches have targeted massive objects with a high far-infrared (FIR) luminosity, $L_{\rm FIR} > 10^{12}\ L_\odot$ (e.g., Maiolino et al. 2005, 2009; Wagg et al. 2010; De Breuck et al. 2011). Recently, the first searches for C II 158 μm emission in LAEs were reported by Walter et al. (2012). In this Letter, we report results from a deep search for C II 158 μm emission in a lensed LAE at $z = 6.56$.

2. HCM 6A: A LENSED LAE AT $z \sim 6.56$

HCM 6A was identified by Hu et al. (2002a) as an LAE at $z = 6.56$ in the field of the $z = 0.375$ galaxy cluster A370. A lensing model for A370 yields a magnification of $\approx$4.5 at the LAE location (Kneib et al. 1993). Hu et al. (2002a) obtained an SFR of $\sim 9\ M_\odot\ {\rm yr^{-1}}$ (see Hu et al. 2002b) from the rest-frame UV continuum, a value typical of the $z \gtrsim 6$ LAE population (e.g., Taniguchi et al. 2005; Cowie et al. 2011). However, a far higher SFR, $\sim 140\ M_\odot\ {\rm yr^{-1}}$, was inferred by Chary et al. (2005) from the excess emission detected in the *Spitzer* 4.5 μm image of the field, suggesting significant dust extinction of the UV continuum. A high SFR, 11–41 $M_\odot\ {\rm yr^{-1}}$, was also obtained by Schaerer & Pelló (2005) by modeling the spectral energy distribution (SED). Conversely, Boone et al. (2007) used a 1.2 mm MAMBO-2 image to obtain a strong constraint on the FIR luminosity, and thence on the SFR, $< 35\ M_\odot\ {\rm yr^{-1}}$. The high magnification factor and the possible high SFR make HCM 6A an excellent target for a search for C II 158 μm emission from a high-z LAE.

3. OBSERVATIONS, DATA ANALYSIS, AND RESULTS

We searched for redshifted C II 158 μm line emission from HCM 6A using five telescopes of the Plateau de Bure Interferometer (PdBI) on 2009 August 18 and 21, with the array in the

[6] Ramanujan Fellow.

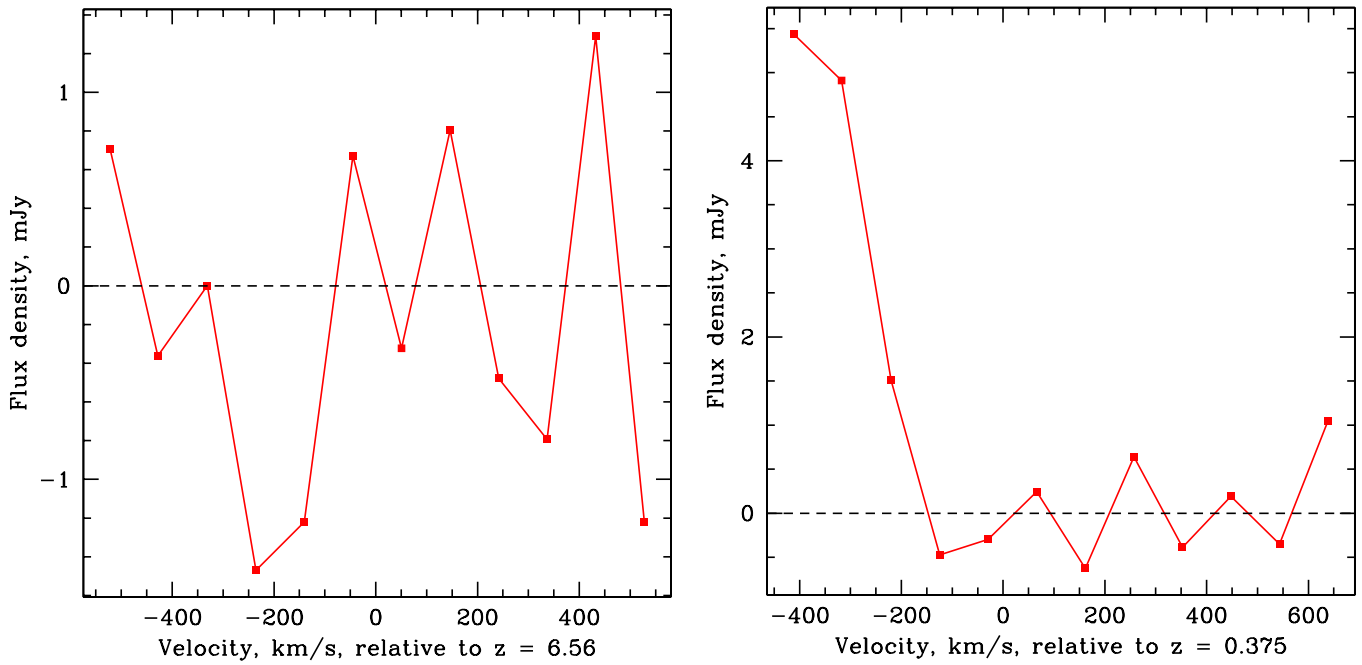

Figure 1. Left panel: the spectrum toward HCM 6A, covering the C II 158 μm line; the velocity scale is relative to the redshifted C II 158 μm line frequency from $z = 6.56$. Right panel: the spectrum obtained from the bright spiral galaxy $\sim 5''$ southwest of HCM 6A; the velocity scale is relative to the redshifted CO $J = 3$–2 line frequency from $z = 0.375$.

(A color version of this figure is available in the online journal.)

compact 5Dq configuration. The observations used a bandwidth of 1 GHz, centered at the redshifted C II 158 μm line frequency of 251.395 GHz, with two orthogonal polarizations and 256 channels. The velocity coverage was $\approx$1200 km s^{-1}, with a velocity resolution of $\approx$4.7 km s^{-1}. This coverage is sufficient to cover errors in the Lyα emission redshift due to Lyα absorption in the intergalactic medium (IGM), as well as scenarios where the Lyα emission arises from outflowing gas (typical velocities of a few hundred km s^{-1} for small galaxies like LAEs).

The complex antenna gains were calibrated on the nearby quasars 0235+164 and 0336−019, the antenna bandpass shapes measured on 3C454.3, and the flux density scale derived from observations of MWC349. The total observing time was 18 hr, in two full-synthesis tracks, with an on-source integration time of 10.5 hr. System temperatures were lower than 200 K during most of the run.

The data were analyzed using standard calibration procedures in the GILDAS[7] package, followed by imaging in the AIPS package. Line-free channels were averaged together to produce a "channel 0" data set for the purpose of continuum imaging; our final continuum map has an angular resolution of $\sim 2\farcs5 \times 1\farcs7$ and an rms noise of 0.16 mJy beam^{-1}. No radio continuum emission was detected in the field.

The final image cube was made using "natural" weighting to maximize the sensitivity, after Hanning smoothing the visibility data and resampling to a velocity resolution of 100 km s^{-1}. No line emission was detected at the location of HCM 6A in the cube, but a strong emission feature was detected $\sim 5''$ southwest of HCM 6A. This was identified as redshifted CO $J = 3$–2 emission from a galaxy in the foreground cluster at $z = 0.375$ (see below). The spectrum obtained at the location of HCM 6A in the CLEANed image cube is shown in the left panel of Figure 1, after smoothing to, and resampling at, a resolution of $\sim$100 km s^{-1}. It has an rms noise of 0.6 mJy per 100 km s^{-1} channel (measured in the image plane).

The optical image of HCM 6A is elongated along a position angle of 110°, with a length of $\sim 4''$ (Hu et al. 2002a). The extended structure is covered by two of our synthesized beams; our limits on the total C II 158 μm luminosity and the 1.2 mm continuum flux density are hence worse by a factor of $\approx\sqrt{2}$ than the limits from a single beam. The non-detections of C II 158 μm line emission and 1.2 mm radio continuum emission from HCM 6A then yield the 3σ upper limits $L_{[\rm C\,II]} < 6.4 \times 10^7 \times (\Delta V/100)^{1/2}\ L_\odot$ on the C II 158 μm line luminosity (assuming a line FWHM of 100 km s^{-1}, typical for small galaxies) and $S_{1.2\,\rm mm} < 0.68$ mJy, after correcting the former for the magnification factor of 4.5.[8]

We also revisited the *Spitzer* photometry of HCM 6A (Chary et al. 2005). Since those results, which used data from *Spitzer* program 64 with an integration time of 2400 s, the field has been observed four times in programs 137 and 60034. We have re-analyzed all of these data, and clearly detected HCM 6A in each epoch. The total exposure time corresponds to more than 10 hours of imaging.

We obtained the post-basic calibrated data mosaics of the HCM 6A field for each program from the *Spitzer* Heritage Archive. The astrometric alignment of each mosaic was assessed through bright sources. Of the three programs, the astrometric alignment of program 60034 appears to be 1.5–2 times worse than the others, with a median offset of $0\farcs4$ relative to the location of the same sources in the Sloan Digital Sky Survey images. Given the high signal-to-noise ratio of the source in each of the mosaics, we simply ignore the frames with worse astrometry rather than applying an astrometric correction to those frames.

[7] http://www.iram.fr/IRAMFR/GILDAS

[8] We use a ΛCDM model with $H_0 = 71$ km s^{-1} Mpc^{-1}, $\Omega_{\rm m} = 0.27$, and $\Omega_\Lambda = 0.73$ (Spergel et al. 2007).

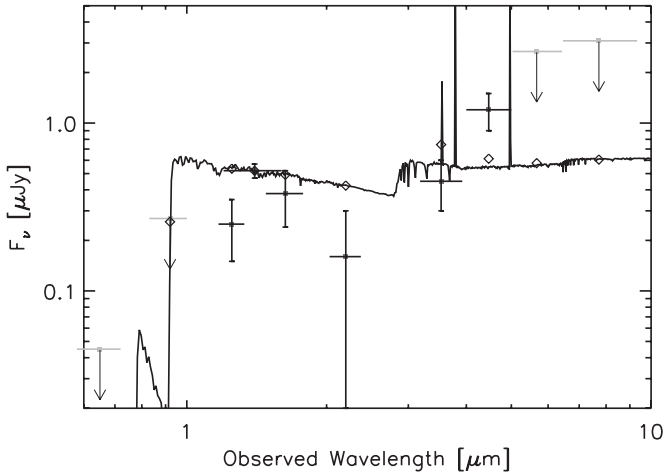

Figure 2. Fit to the SED of HCM 6A at rest-frame UV to optical wavelengths, with a modified sub-solar ($Z = 0.2\ Z_\odot$) metallicity BC03 model. The points with error bars are the various measurements, while the open diamonds indicate values from the best-fit model. See the text for discussion.

The 3.6 μm and 4.5 μm photometry of HCM 6A was carried out both in the mosaics from the individual *Spitzer* observations, as well as from a super-mosaic of all the data with good astrometry. The super-mosaic was constructed using SWARP, via an integration-time-weighted median combination of the mosaics with good astrometry.

Due to the contamination of the flux density of HCM 6A by the bright extended spiral galaxy 5″ to the southwest, we used GALFIT to model the spatial profile of the spiral and subtract it out. HCM 6A's flux density in the different mosaics spans the range 0.3–0.6 μJy at 3.6 μm and 1–1.4 μJy at 4.5 μm, with systematics from the subtraction of the spiral dominating the errors. The statistical uncertainty of the flux density values is 0.1 μJy.

We used a modified version of the Bruzual & Charlot (2003; BC03) population synthesis models to fit the complete SED of HCM 6A over the rest-frame UV to the optical wavelength range using our *Spitzer* measurements, the recent 1.4 μm detection (Cowie et al. 2011), and the data of Hu et al. (2002a). Our modification of the BC03 model involved the inclusion of nebular line emission, particularly of the energetically important Lyα, [O II], Hβ, [O III], Hα, and [N II] lines. The relative line ratios correspond to those observed in nearby Hα emitters, which have been argued to be local analogs of high-z star-forming galaxies (Shim & Chary 2013). The absolute line strengths were calibrated with respect to the far-UV (FUV) continuum at 1500 Å derived from the BC03 models. Since nebular line emission is correlated with Lyman continuum emission and not FUV continuum emission, this is potentially an inaccurate assumption. We added these emission lines to the BC03 templates for stellar photospheric emission and then fit the multi-wavelength photometry, taking the IGM absorption into account. The high signal-to-noise ratio of the photometry in Cowie et al. (2011) drives the best-fit model, as shown in Figure 2; this does a poor job of reproducing the *Spitzer* photometry. While the excess emission in the 4.5 μm band suggests Hα contamination (Chary et al. 2005), the *Spitzer* photometry is affected by systematics due to source confusion with the foreground spiral. Our best-fit SED model yields a stellar mass of $1.3 \times 10^9\ M_\odot$ and an SFR of $\approx 10\ M_\odot\ \mathrm{yr}^{-1}$ for HCM 6A, with negligible dust obscuration.

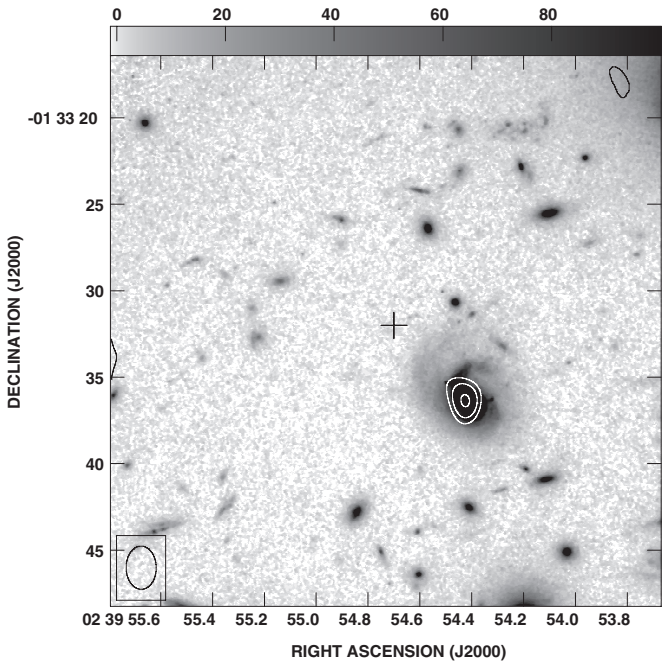

Figure 3. Overlay of the integrated CO $J = 3$–2 emission (in contours) on the *HST*/ACS optical image (in gray scale). The emission feature arises from the bright spiral, 5″ southwest of HCM 6A, whose position is marked by a "+" sign.

The CO $J = 3$–2 spectrum obtained toward the $z = 0.375$ galaxy in A370 is shown in the right panel of Figure 1, again at a resolution of ∼100 km s^{-1}, but with the velocity scale relative to the redshifted CO $J = 3$–2 line frequency at $z = 0.375$. Figure 3 shows an overlay of the integrated emission (in contours) on an optical image from the Advanced Camera for Surveys (ACS) on board the *Hubble Space Telescope* (*HST*) in the F814W band (Richard et al. 2010). The emission feature clearly arises from the bright cluster galaxy 5″ to the southwest of HCM 6A. Unfortunately, the feature is right at the edge of our observing band, with part of the emission outside the band. We hence obtain a *lower limit* to the line flux of 1.13 ± 0.10 Jy km s^{-1}, after CLEANing the cube. Assuming that the CO $J = 3$–2 line is thermalized, this implies a CO line luminosity of $L'(\mathrm{CO}) > (8.95 \pm 0.79) \times 10^8$ K km s^{-1} pc^2.

4. DISCUSSION

It has been suggested that the C II 158 μm line luminosity might be used to estimate the SFR in star-forming galaxies (e.g., Stacey et al. 1991; Boselli et al. 2002; de Looze et al. 2011), unbiased by dust extinction. De Looze et al. (2011) found a good correlation between the C II 158 μm line luminosity and the SFR (determined from a combination of the FUV continuum and the 24 μm continuum magnitudes) for 24 nearby star-forming galaxies, with $\log[\mathrm{SFR}_{[\mathrm{FUV+24\,\mu m}]}/(M_\odot\ \mathrm{yr}^{-1})] = 0.983 \times \log[\mathrm{L}_{[\mathrm{C\,II}]}/(\mathrm{erg\ s}^{-1})] - 40.012$. The relation, which has a 1σ dispersion of 0.27 dex, is expected to be applicable to star-forming galaxies with SFR ∼ 0.05–127 $M_\odot\ \mathrm{yr}^{-1}$.

Our non-detection of C II 158 μm emission in HCM 6A gives $L_{[\mathrm{C\,II}]} < 6.4 \times 10^7 (\Delta V/100)^{1/2}\ L_\odot$. This is a significantly tighter constraint than that obtained by Walter et al. (2012) in two LAEs at $z \approx 6.6$–7.0, mostly due to the large magnification factor in HCM 6A. Using the relation of de Looze et al. (2011), this implies an upper limit of ∼4.7 $M_\odot\ \mathrm{yr}^{-1}$ to the total SFR (both obscured and unobscured). However, the lower limit to the SFR from the UV continuum is ∼9 $M_\odot\ \mathrm{yr}^{-1}$, a factor of ∼2 higher

than the above upper limit. Further, the discrepancy between the predicted and observed SFRs would be exacerbated if dust extinction is indeed significant in the LAE (Chary et al. 2005; Schaerer & Pelló 2005). Our results thus suggest that the local relation between the C II 158 μm line luminosity and SFR may not be applicable to high-z LAEs (although we note that the dispersion in the local relation is a factor of $\approx$1.9).

Our upper limit to the 1.2 mm radio continuum flux density of HCM 6A (0.68 mJy) is slightly tighter than that of Boone et al. (2007; 1.08 mJy). Since the observing frequency of 1.2 mm corresponds to a rest frequency of 158.6 μm at $z = 6.56$, we will use the conversion factor of Calzetti et al. (2010; valid for star-forming and starburst galaxies) to convert the 160 μm luminosity to an SFR. We obtain a 3σ upper limit of 28 $M_\odot$ yr^{-1} on the SFR, after including the lensing factor of 4.5. This is within a factor of three of the SFR derived from the UV continuum (Hu et al. 2002a), indicating that any obscured star formation in HCM 6A is at most two times larger than the visible star formation. Using the same assumptions as Boone et al. (2007) yields a 3σ SFR upper limit of 22 $M_\odot$ yr^{-1}, and does not significantly change the above result.

Our best-fit SED model yields an SFR of $\approx$10 $M_\odot$ yr^{-1}, consistent with the SFR estimates from the UV continuum and the upper limit to the 1.2 mm continuum flux density. Chary et al. (2005) inferred a far higher SFR (140 $M_\odot$ yr^{-1}) from the excess 4.5 μm emission, assuming this arises from Hα contamination. However, the SFR derived from the Hα line flux critically depends on the age of the stellar population. If HCM 6A is indeed similar in physical properties to the $z \sim 5$ Hα emitters reported in Shim et al. (2011) and the local Hα emitters of Shim & Chary (2013), then the photometry is dominated by a population of massive O stars, which excite Hα emission due to their strong ionizing photon field. In such a situation, the same Hα line flux corresponds to a *lower* SFR than that obtained from the standard calibration (Kennicutt 1998). Thus, depending on the age of the stellar population, the same Hα line flux could correspond to an SFR in the range of 30–150 $M_\odot$ yr^{-1}.

The ratio of a galaxy's luminosity in the Hα and FUV bands is a sensitive tracer of the properties of the stellar population, including its metallicity, initial mass function (IMF), and age, and the extent of dust obscuration (e.g., Kennicutt 1998; Shim et al. 2011). We note that the SFR estimates from the UV continuum and the Hα line are only valid for a Salpeter IMF and a 100 Myr continuously star-forming stellar population. At low ages (<10 Myr), there are more Lyman continuum and UV photons produced per unit baryon in stars; a lower SFR can thus yield a higher Hα/UV flux ratio. Comparing the observed ratio in high-z LAEs with predictions from population synthesis models thus provides insights on early stellar populations. We have investigated this via a simulation in *Starburst99* (Leitherer et al. 1999), using constant star formation models (SFR = 1 $M_\odot$ yr^{-1}) with a range of metallicities ($0.02 < Z/Z_\odot < 1$) and IMFs. In HCM 6A, the measured Hα/FUV ratio is $\approx$0.03–0.16, including systematic errors in the Hα luminosity; this is consistent with values expected from low-metallicity young stellar populations with a top-heavy IMF (see Figure 4). However, the intrinsic ratio could be lower than this if dust preferentially obscures the FUV continuum. Combining our upper limit on the 1.2 mm flux density with the FUV photometry yields a lower limit of 0.02 on the Hα/FUV ratio, and thus an allowed range of 0.02–0.16, marginally consistent with values expected from standard stellar populations and IMFs at low metallicity. Note that increasing the SFR would cause the four curves to shift toward the right. While a young (<1 Myr) starburst can explain the observed ratio, such an age is unlikely due to the low probability of detecting such a young starburst at a time when the universe is $\gtrsim$1 Gyr old.

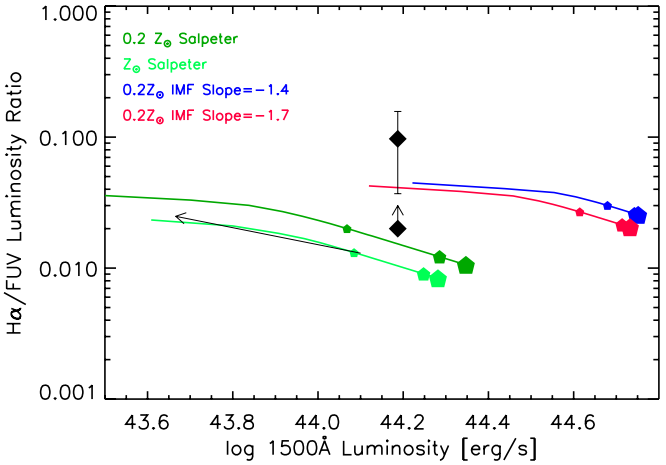

Figure 4. Temporal evolution of the ratio of Hα to FUV flux for different stellar populations, evaluated using *Starburst99*; the stars of increasing size are at 0.01, 0.1, and 1 Gyr, and the arrow shows 1 mag of extinction at 1500 Å. The lowest two curves are for Salpeter stellar populations with solar and 0.2 solar metallicity, respectively, while the top two curves are for populations with 0.2 solar metallicity, but IMF slopes of -1.4 and -1.7. The two diamonds indicate the value of the Hα/FUV flux ratio in HCM 6A, the upper one giving the measured ratio, and the lower one accounting for possible dust obscuration of the FUV continuum (see the main text).

For the galaxy detected in CO $J = 3$–2 emission, assuming a CO-to-H_2 conversion factor allows us to infer its molecular gas mass. The $z = 0.375$ galaxy has been classified as a spiral by Mellier et al. (1988), based on its optical colors. We hence use the Milky Way conversion factor $X_{\rm CO} = 4.6\,M_\odot$ (K km s^{-1} pc^{-2})$^{-1}$ (Solomon & Barrett 1991) to obtain $M({\rm H_2}) > (4.12 \pm 0.36) \times 10^9\,M_\odot$. This assumes that the CO $J = 3$–2 transition is thermalized. However, Dannerbauer et al. (2009) find that large spiral galaxies at $z \sim 1.5$ have sub-thermal CO $J = 3$–2 line emission, similar to the situation in the Galaxy (e.g., Fixsen et al. 1999). Our estimate thus provides a lower limit to the molecular gas mass because (1) the CO $J = 3$–2 emission may be sub-thermal and (2) part of the CO emission lies outside our observing band. Finally, we do not spatially resolve the CO emission, indicating that it arises from a region smaller than $\sim$9 kpc $\times$13 kpc.

The $z = 0.375$ galaxy (BO 39) is located $\approx$330 kpc from the cluster center, well within the cluster virial radius ($\approx$2.6 Mpc); it has a velocity of +100 km s^{-1} relative to $z = 0.374$ (Mellier et al. 1988). The detection of CO emission from a galaxy close to the center of a large cluster allows a test of whether ram pressure stripping can denude a galaxy of its molecular gas, as is believed to occur for the atomic gas (e.g., Gunn & Gott 1972; Chung et al. 2007). We note that the CO line emission peaks at $z \approx 0.373$, while the galaxy redshift is $z = 0.3745$ (Mellier et al. 1988). Follow-up mapping CO $J = 1$–0 studies will be of much interest.

5. SUMMARY

We report strong constraints on the C II 158 μm line luminosity and the 1.2 mm radio continuum flux density of the $z = 6.56$ LAE, HCM 6A, from a PdBI imaging study. The C II 158 μm non-detection suggests that the local conversion factor from

C II 158 μm line luminosity to SFR may not be applicable to high-z galaxies. Our upper limit to the SFR from the 1.2 mm continuum non-detection indicates that the LAE does not have significant obscured star formation. Our best-fit model to the SED of HCM 6A yields a stellar mass of $1.3 \times 10^9\ M_\odot$ and an SFR of $\approx 10\ M_\odot\ \mathrm{yr}^{-1}$, with negligible dust obscuration. This is consistent with the SFR estimates from the UV continuum and the 1.2 mm radio continuum. We detect CO $J = 3$–2 emission from a $z = 0.375$ spiral galaxy in the foreground cluster A370, and obtain the lower limit $M(\mathrm{H_2}) > (4.12 \pm 0.36) \times 10^9\ M_\odot$ on its molecular gas mass.

N.K., J.W., and C.C. are grateful for support from the Max-Planck Society and the Alexander von Humboldt Foundation. N.K. acknowledges support from the Department of Science and Technology through a Ramanujan Fellowship. The National Radio Astronomy Observatory is a facility of the National Science Foundation operated under cooperative agreement by Associated Universities, Inc.

REFERENCES

Boone, F., Schaerer, D., Pelló, R., Combes, F., & Egami, E. 2007, A&A, 475, 513
Boselli, A., Gavazzi, G., Lequeux, J., & Pierini, D. 2002, A&A, 385, 454
Bruzual, G., & Charlot, S. 2003, MNRAS, 344, 1000
Calzetti, D., Wu, S.-Y., Hong, S., et al. 2010, ApJ, 714, 1256
Carilli, C. L., & Walter, F. 2013, ARA&A, in press (arXiv:1301.0371)
Chary, R.-R., Stern, D., & Eisenhardt, P. 2005, ApJL, 635, L5
Chung, A., van Gorkom, J. H., Kenney, J. D. P., & Vollmer, B. 2007, ApJL, 659, L115
Cowie, L. L., Hu, E. M., & Songaila, A. 2011, ApJL, 735, L38
Crawford, M. K., Genzel, R., Townes, C. H., & Watson, D. M. 1985, ApJ, 291, 755
Dannerbauer, H., Daddi, E., Riechers, D. A., et al. 2009, ApJL, 698, L178
De Breuck, C., Maiolino, R., Caselli, P., et al. 2011, A&A, 530, L8
de Looze, I., Baes, M., Bendo, G. J., Cortese, L., & Fritz, J. 2011, MNRAS, 416, 2712
Fixsen, D. J., Bennett, C. L., & Mather, J. C. 1999, ApJ, 526, 207
Gunn, J. E., & Gott, J. R., III. 1972, ApJ, 176, 1
Hu, E. M., Cowie, L. L., McMahon, R. G., et al. 2002a, ApJL, 568, L75
Hu, E. M., Cowie, L. L., McMahon, R. G., et al. 2002b, ApJL, 576, L99
Kashikawa, N., Shimasaku, K., Matsuda, Y., et al. 2011, ApJ, 734, 119
Kennicutt, R. C., Jr. 1998, ApJ, 498, 541
Kneib, J. P., Mellier, Y., Fort, B., & Mathez, G. 1993, A&A, 273, 367
Leitherer, C., Schaerer, D., Goldader, J. D., et al. 1999, ApJS, 123, 3
Maiolino, R., Caselli, P., Nagao, T., et al. 2009, A&A, 500, L1
Maiolino, R., Cox, P., Caselli, P., et al. 2005, A&A, 440, L51
Mellier, Y., Soucail, G., Fort, B., & Mathez, G. 1988, A&A, 199, 13
Pierini, D., Lequeux, J., Boselli, A., Leech, K. J., & Völk, H. J. 2001, A&A, 373, 827
Richard, J., Kneib, J.-P., Limousin, M., Edge, A., & Jullo, E. 2010, MNRAS, 402, L44
Schaerer, D., & Pelló, R. 2005, MNRAS, 362, 1054
Shim, H., & Chary, R.-R. 2013, ApJ, 765, 26
Shim, H., Chary, R.-R., Dickinson, M., et al. 2011, ApJ, 738, 69
Solomon, P. M., & Barrett, J. W. 1991, in IAU Symp. 146, Dynamics of Galaxies and Their Molecular Cloud Distributions, ed. F. Combes & F. Casoli (Dordrecht: Kluwer), 235
Spergel, D. N., Bean, R., Doré, O., et al. 2007, ApJS, 170, 377
Stacey, G. J., Geis, N., Genzel, R., et al. 1991, ApJ, 373, 423
Stacey, G. J., Hailey-Dunsheath, S., Ferkinhoff, C., et al. 2010, ApJ, 724, 957
Taniguchi, Y., Ajiki, M., Nagao, T., et al. 2005, PASJ, 57, 165
Wagg, J., Carilli, C. L., Wilner, D. J., et al. 2010, A&A, 519, L1
Wagg, J., & Kanekar, N. 2012, ApJL, 751, L24
Wagg, J., Kanekar, N., & Carilli, C. L. 2009, ApJL, 697, L33
Walter, F., Bertoldi, F., Carilli, C., et al. 2003, Natur, 424, 406
Walter, F., Decarli, R., Carilli, C., et al. 2012, ApJ, 752, 93
Wang, R., Carilli, C. L., Neri, R., et al. 2010, ApJ, 714, 699
Wang, R., Wagg, J., Carilli, C. L., et al. 2011, ApJL, 739, L34
Wolfire, M. G., Hollenbach, D., McKee, C. F., Tielens, A. G. G. M., & Bakes, E. L. O. 1995, ApJ, 443, 152